



CFD ELECTRIC MOTOR EXTERNAL FAN SYSTEM COMPARISON AND VALIDATION

Cassiano A. CEZARIO

*Research and Technological Innovation Department, WEG Equipamentos
Eletricos – Motores, Av. Prefeito Waldemar Grubba, 3000, Malote 41,
89256-900, Santa Catarina, Brazil*

SUMMARY

The work that involves numerical simulation usually requires the adoption of both geometric and physical simplifications. The impact of such simplifications usually appears when experimental and numerical data are compared, once those eventual disagreements between them are invariably attributed to these factors. With the objective of just evaluating the performance of the CFD software an experimental device, based on Totally Enclosed Fan Cooled (TEFC) electric motor was especially developed. With this approach it was possible to concentrate the efforts in numerical problems and evaluate traditional CFD questions, such as: turbulence models, impact of y^+ , mesh size, interface treatments, among others.

INTRODUCTION

This work presents a comparison between different approaches that can be used to evaluate the external fan system of an electric motor in a Computational Fluid Dynamics (CFD) code. The entire process of comparison was supported by the experimental data, which was obtained from a special device. This device was designed and manufactured in order to consider a number of geometric simplifications aiming the validation of a CFD model. The geometry of the experimental device was transposed to commercial Computer Aided Design (CAD) software with insignificant adjustments, only when it was extremely necessary, to avoid numerical problems in CFD software. With this approach it was possible to concentrate the efforts in numerical problems, avoiding questions like, were the differences between numerical and experimental data originated by numerical error or geometrical considerations?

From numerical point of view the impact of turbulence model is a critical point in CFD simulations, so the turbulence model Shear Stress Turbulence (SST) and $k-\epsilon$ were confronted, both based on Reynolds Average Navier-Stokes (RANS). Especial attention was dedicated to the variation of the y^+ , i.e., quality of the mesh near the wall. Additionally, the problems of numerical convergence in steady-state regimes were discussed in this work. The numerical results were confronted with air velocity and fan power consumption, both experimentally obtained, and showed good agreement in external flow.

EXPERIMENTAL DATA

During the conception and production phases of the experimental device it was intended to incorporate as many geometric simplifications as possible, as well as the cyclical periodicity concept, in order to transpose the physical geometry to the numerical domain with the highest fidelity possible. For this reason and with the objective of just evaluating the performance of CFD software, a special device [1] was developed.

Basically, an especial frame with no connection box was produced, making more feasible the assumption of the hypothesis of cyclical periodicity, Figure 1a and 1b. Another significant difference between the analyzed motor and a standard one concerns the fan cover, which had the bars of its air entrance removed in the case of the analyzed motor, Figure 1c and 1d. In Figure 1f, it is possible to observe that the end shield does not have any saliencies or reentrances, different of standard end shield (Figure 1e).

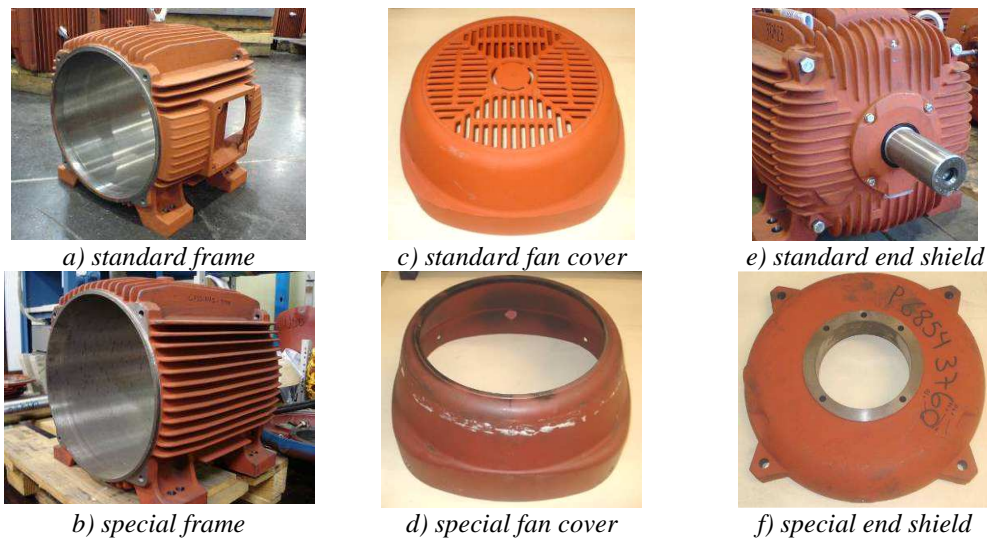


Figure 1: special device to CFD validation

The experimental device used in this study is presented in Figure 2. All these modifications were made to simplify the process of mesh generation, consequently reducing the computational processing time and increasing the authenticity of the Computer Aided Design (CAD) model.



Figure 2: experimental device

Two experimental parameters were chosen to be compared with the numerical results, the air velocity between the external fins and the consumption of energy by the external fan system.

The air velocity was measured between the fins in 13 measurement points in the transverse direction, Figure 3a, in four longitudinal planes (A, B, C and D), Figure 3b, totalizing 52 points.

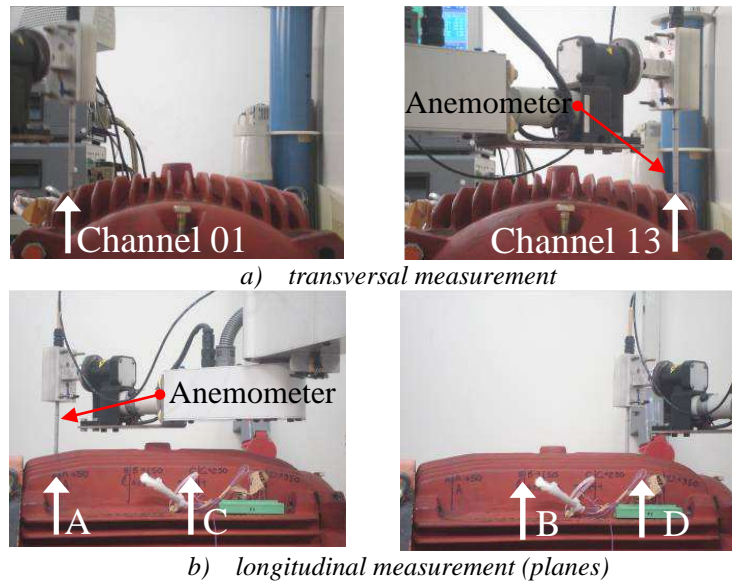


Figure 3: air velocity measurement points

For data acquisition, a TSI anemometer of the 8465 model was used. Figure 4a presents the anemometer and a comparison with a 0.5 mm mechanical pencil. Figure 4b illustrate the anemometer in plane D, channel 07, while the measurement process.

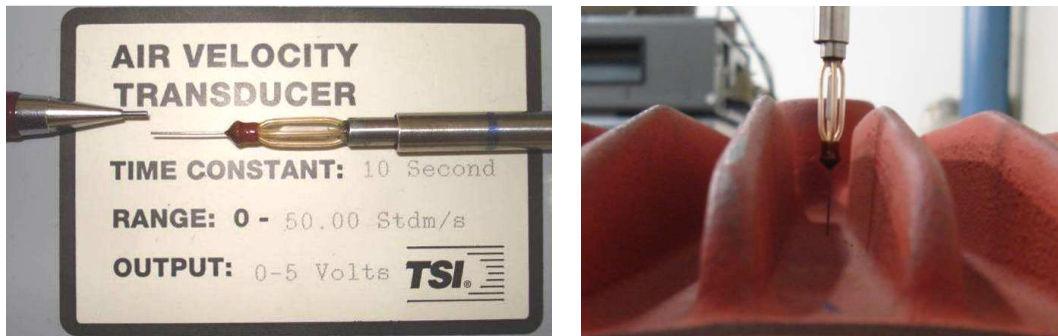


Figure 4: anemometer and measurement chain details

To determine the consumption of energy by the fan system, it was necessary to use an auxiliary electric motor, once that the special device was not capable of rotating its own rotor. A power analyzer was used to measure the energy supplied to the auxiliary electric motor. The consumption of energy by the external fan system was obtained from the differences found between the data measured during tests accomplished with and without the fan. A general view of the apparatus used to measure the consumption of energy by the fan system is shown in Figure 5.

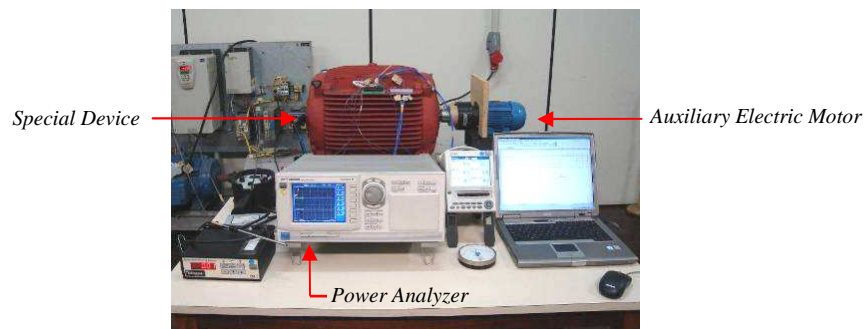


Figure 5: determination of energy consumption by the fan system

NUMERICAL ANALYSIS

Geometric Simplifications

The unique exception in the transposition from physical to numerical domain were the removal of radii in the corner of fins, the elimination of screws, and the addition of a surface between the place where the end shield is attached to the frame and the frame itself, as shown in Figure 6. This simplification had the objective of simplifying the process of mesh generation.

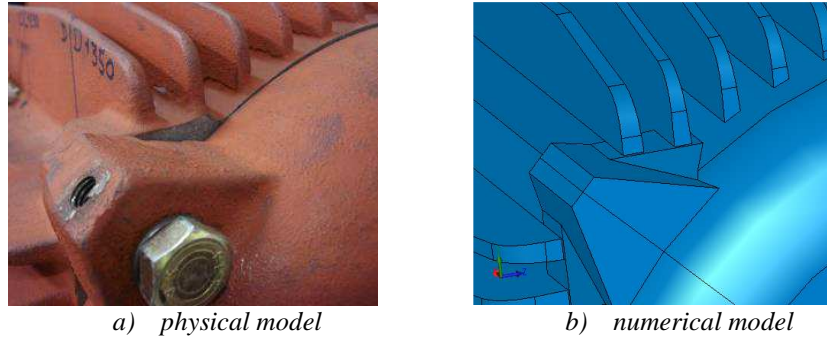


Figure 6: geometric simplifications

Figure 7 presents the physical and numerical model that was used in the most evaluations. It is possible to observe that numerical model take advantage of using the concept of cyclical periodicity, only 1/4 of the geometry of the motor was numerically modeled.

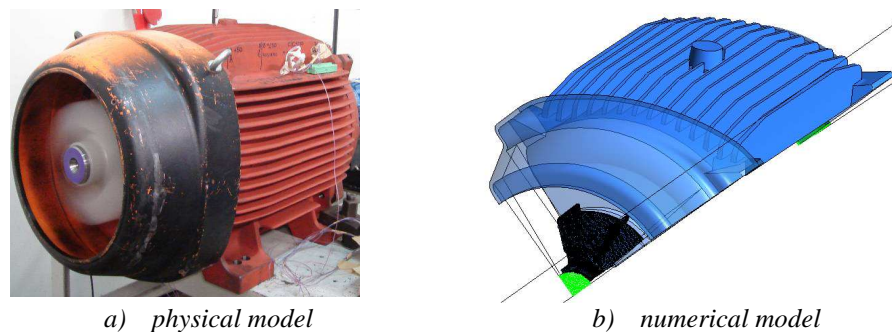


Figure 7: physical versus numerical model

Turbulence models

Unfortunately up to now the most CFD users do not have computational resources to evaluate directly all scale of motion. Basically the correlation of the mesh size and Reynolds number to solve a Direct Navier-Stokes (DNS) or, at the same, Large Eddy Simulation (LES) for an industry problem can easily exceed billions of nodes and demand months of simulation. This scenario leads to steady-state solution and Reynolds Average Navier-Stokes (RANS) models. The most used and broadcast RANS model is $k-\epsilon$ and its variations. Unfortunately this model has positive and negative aspects. Another model is $k-\omega$ that basically has opposite aspects, when compared to $k-\epsilon$. Observing the difference between models Menter [2] proposed in 1993 the Shear Stress Turbulence (SST), which is basically a blend of the best characteristics of $k-\epsilon$ and $k-\omega$. Additionally to the implementation of SST in CFX the Automatic Wall Treatment was added. Using a blend function the Automatic Wall Treatment allows a smooth shift from a low-Reynolds number form to a wall function formulation. Table 1 presents a simplified comparison between this traditional turbulence models and SST.

Table 1: turbulence models

Turbulence model	k-ε	k-ω	SST
Flow separation point	underestimate	realistic	realistic
Near wall flow	inaccurate	good precision	good precision
Free-stream	robust	unstable	robust
Wall treatment	scalable (cfx)	resolution of ω	automatic

It is important emphasize that the wall function adopted to k-ε in CFX is Scalable and recommended values of y^+ to this model is between 20 and 200. Values of y^+ lower than 11.06 are disregard and consequently the mesh nodes under this limit value, Vieser [3]. The value of 11.06 marks the intersection between the logarithmic and linear profile and has the objective of avoid positioning of mesh nodes inside of linear profile. To SST and Automatic Wall Treatment an important recommendation is a minimal number of 15 nodes inside of boundary layer and the value of $y^+ \leq 2$.

Convergence criterion

During the solution of the numerical problem an analysis in steady-state regime was tried, but the convergence criteria, $1.0e^{-5}$ (rms) [4], was not achieved. By means of a detailed analysis of the results based on the location of the maximum residual values (Figure 8a) and the airflow characteristics (Figure 8b), it was possible to observe that the difficulty in getting convergence was directly related to the presence of recirculation structures in the front area of the motor.

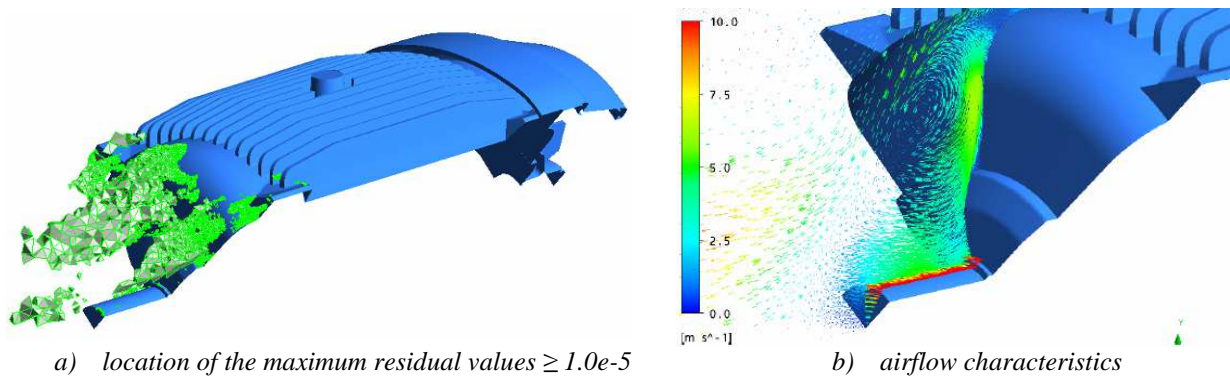


Figure 8: airflow fluctuations

However, the area of interest was located between the frame fins and not in the front area of the motor. For this reason, air velocity monitoring points were inserted between the fins, Figure 9.

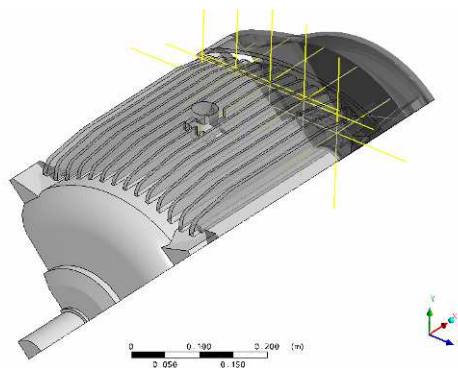


Figure 9: monitoring points between fins

The air velocity values in the monitoring points were observed and their stabilization was adopted as convergence criteria. It is important to observe in Figure 8 that the periodic behavior of residuals occurs around iteration 240, whereas the stabilization of air velocity occurs only after iteration 320, Figure 10. A subsequent analysis of the values of residuals between the fins indicated that the recommended convergence criteria [4] were attended.

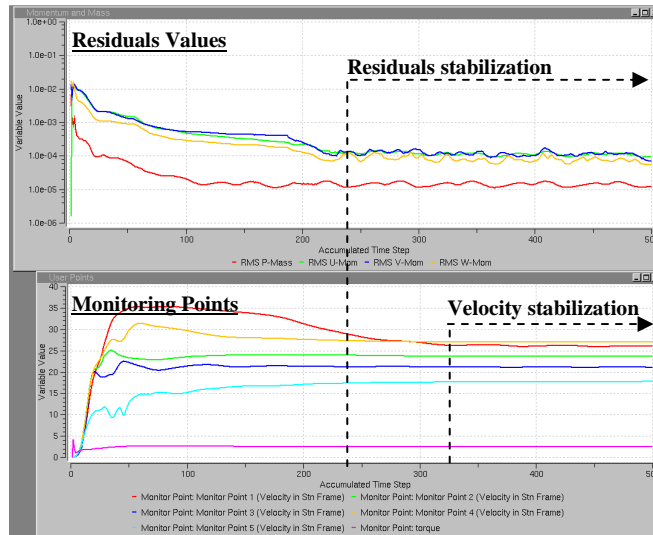


Figure 10: monitoring of air velocity stabilization and residuals values

It is important to emphasize that this methodology assumes that the recirculation zone in front of the motor do not affect the flow field far, i.e., monitoring points and between fins. This assumption can be considered reasonable because the location of residuals higher than $1.0e^{-5}$ (rms) are located only in front of the motor in different time steps (Figure 8a).

Boundaries conditions

Basically the boundaries conditions adopted were the atmospheric pressure on far field, that was positioned distant 3 m of electric motor surface (Figure 11) and the rotating velocity (3600 rpm) to the domain of the fan.

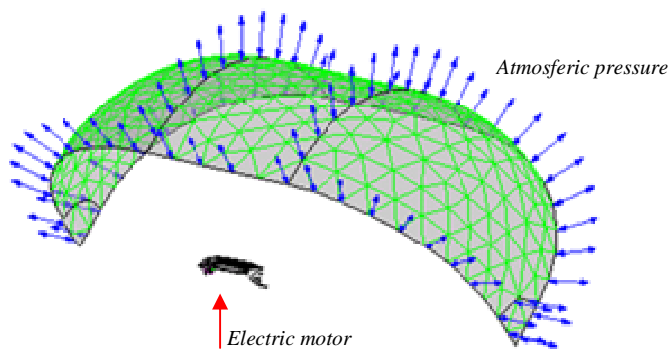


Figure 11: far field boundary condition

Comparison criteria

The comparison criteria adopted was the evaluation of the air velocity between fins, in each channel, and in plane C and D (Figure 3). The choice of these planes is due to the abrupt air velocity variations in central channels, generated by the eyebolt base. Figure 12 presents the experimental and numerical air velocity data acquisition.

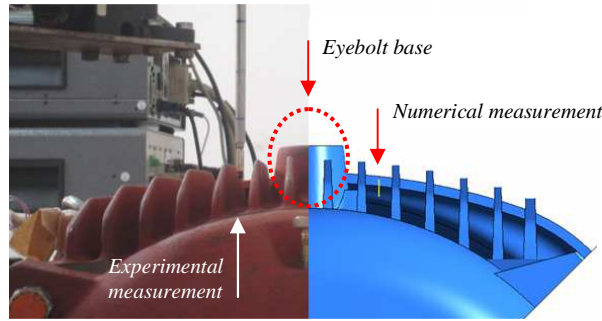


Figure 12: air velocity measure, experimental versus numerical

Computational resources

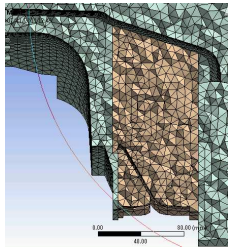
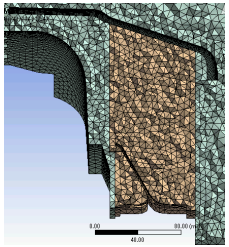
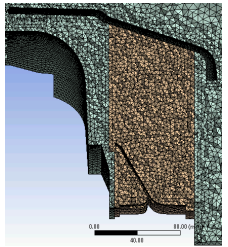
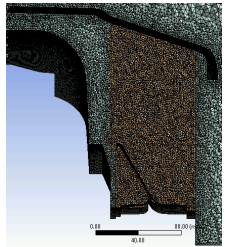
For all simulations, CAD software adopted was SolidWorks 2009 SP2.1 and the CFD software was ANSYS-CFX 13.0 SP2. The simulation process was made in two HP Z800 Workstations with two Xeon X5690 (six-core) processors and 24 GB memory each.

RESULTS

Mesh size

The first evaluation was the determination of volumetric mesh at and near the surface of the electric motor. To lead this evaluation the experimental value of torque was used, although another global parameter, like mass flow, can be used. Essentially four sizes of mesh were adopted and when error values compared to the experimental data were lower than 10 %, the process was interrupted. Table 2 correlate essential parameters involved in mesh size evaluation and illustrate the impact of mesh size at volumetric mesh in the region of fan and fan cover.

Table 2: Mesh size

Mesh size	8 mm	6 mm	4 mm	2 mm
Mesh illustration				
Number of nodes	74 769	124 439	313 177	1 473 722
Processing time ¹	709 s	887 s	1 595 s	6 079 s
Torque error – SST	47.9 %	48.1 %	16.9 %	6.9 %
Torque error – k-ε	54.9 %	overflow	overflow	overflow

¹ Solver wall clock in CFX.

During the simulations, k-ε resulted in the crash of the software, denominated *overflow* in Table 1. A possible interpretation for this is the small number of elements across the gap between interface and the wall. However, the same mesh was used for SST and k-ε, fact that leads to the possibility that the use of Low-Reynolds/Automatic Wall Treatment makes SST more robust.

Prisms

To obtain an adequate solution and attend to the orientations of CFX [5] to different turbulence models, wall regions received prisms layer in all surfaces. All mesh adopted the size of 2 mm to volumetric mesh at and near the wall, as defined in previous item. Table III presents a global vision of the prism parameters evaluated and the total processing time necessary to solve each case with different turbulence model. Based on results of Table 3 it was possible to conclude that k- ϵ was faster than SST, especially if we remember that the mesh was oversized to the k- ϵ , based on recommended range of y^+ that was between 20 and 200 and the limit of y^+ equal to 11.06 due to Scalable Wall Function.

Table 3: Prism parameters

Case	A	B	C	D	E	F
Number of nodes	5 730 158	3 681 182	2 871 721	4 155 898	3 890 723	1 904 273
Number of layers	19	11	6	11	11	without
Dimension of 1st layer	0.03 mm	0.03 mm	0.03 mm	0.03 mm	0.15 mm	without
Growth rate	1.15	1.50	2.59	1.20	1.20	without
y^+ (mean value)	1.88	1.81	1.77	1.85	9.15	45.91
Processing time¹ - SST	10 594 s	--- ²	--- ²	8 901	8 462 s	6 494 s
Processing time¹ - k-ϵ	10 435 s	7 907 s	6 209 s	8 698	7 958 s	Overflow

¹ Solver wall clock in CFX. ² No measure was made.

Influence of the number of layers

CFX [4] emphasizes the importance of resolving the boundary layer with at least 10 nodes for models that use wall function or scalable function in the case of k- ϵ . For models based in low-Reynolds, like SST, the recommendation was a minimum of 15 nodes.

For this evaluation, values obtained from cases A, B, and C from Table III will be used, Figure 12. It is important to observe that these cases had the same size for the first layer. The number of layers and growth rate are changing. A good estimation for the size of the first element can be made starting from the Reynolds number for plane plate [4]. Simultaneous were presented the comparison between turbulence models SST and k- ϵ .

Based on results presented in Figure 12 it is possible to conclude that for SST an adequate discretization of boundary layer is fundamental to the accuracy of the results, and it is interesting to observe that the values predicted are in the most cases lower than experimental values. For k- ϵ it was observed that the values obtained from numerical simulation are over predicted.

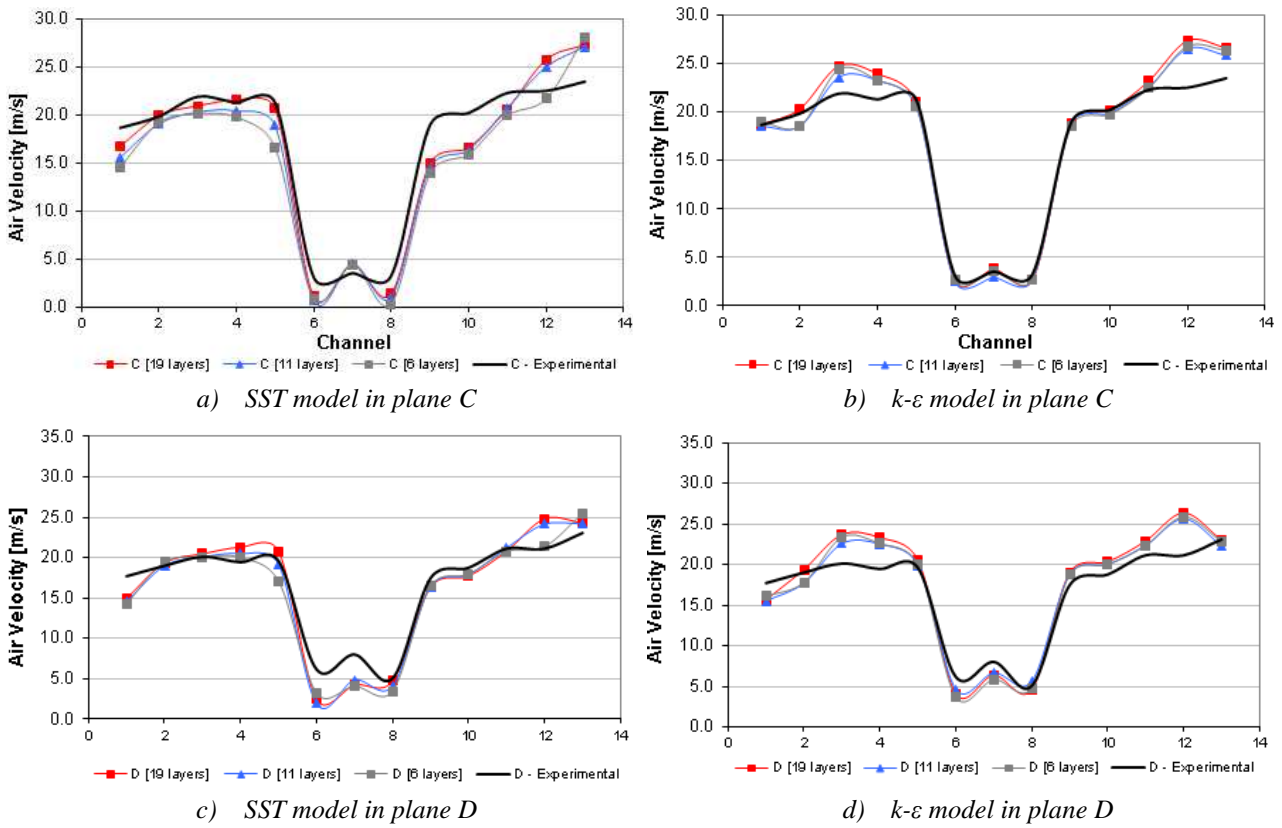


Figure 12: Air velocity comparison for number of layers

Influence of y^+

For this evaluation, values obtained from cases D, E, and F from Table III will be used. The variation of y^+ was obtained from the variations of first layer size, for cases E and F, and due to the absence of prisms layers to case F. Figure 13 presented the comparison between turbulence models SST and k-ε.

Based on results presented in Figure 13 it is possible conclude that for SST the adequate prediction of the y^+ value, lower than 2, was fundamental to obtain reliable results. The Automatic Wall Treatment with values bigger than 2 impacts in the accuracy of the results, at least for this evaluation. For k-ε it was not observed significant variations, however it is necessary to remember that these models fall back on the Scalable Wall Function. This means that in all evaluated cases the real value of y^+ was limited in 11.06, which was a limit, imposed by Scalable Wall Function. Again was observed that the values obtained from numerical simulation are over predicted.

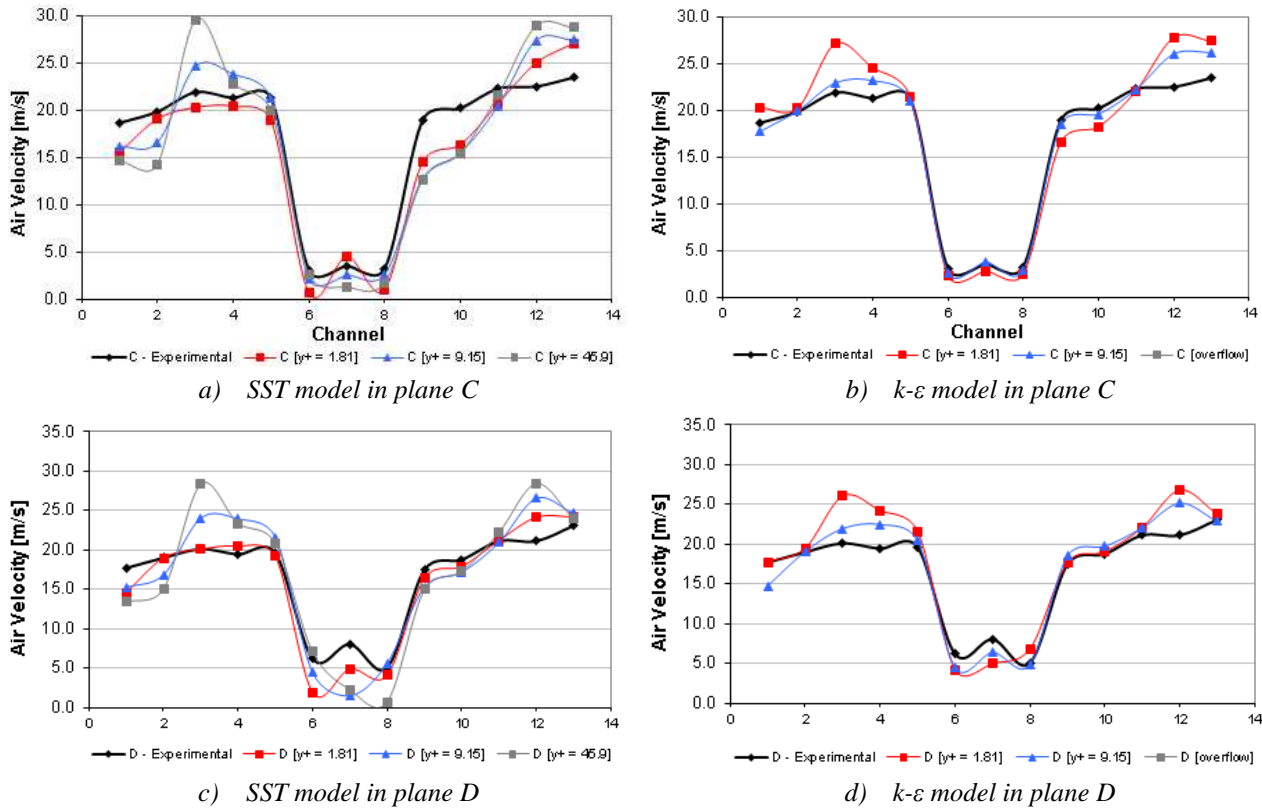


Figure 13: Air velocity comparison for y^+

SST – Blend function

The most commonly definition of SST model is that this is a blend of a $k-\omega$ model, used near the walls, and a $k-\epsilon$ model in regions far from walls. However, one of the most important parameter is the shear stress transport component, which denominates the model. In CFX it is possible, by the second blending function for SST, to verify which model was used in which region. Figure 14 presents the distribution of the turbulence models in a plane for two different values of y^+ . It was to possible verifying the transition from $k-\omega$ (1.00) to $k-\epsilon$ (0.00). In these figures it is also possible to observe a direct dependence with the mesh, while in Figure 14a all regions of the fins were calculated with the $k-\omega$ model in Figure 14b a transition was present between the fins.

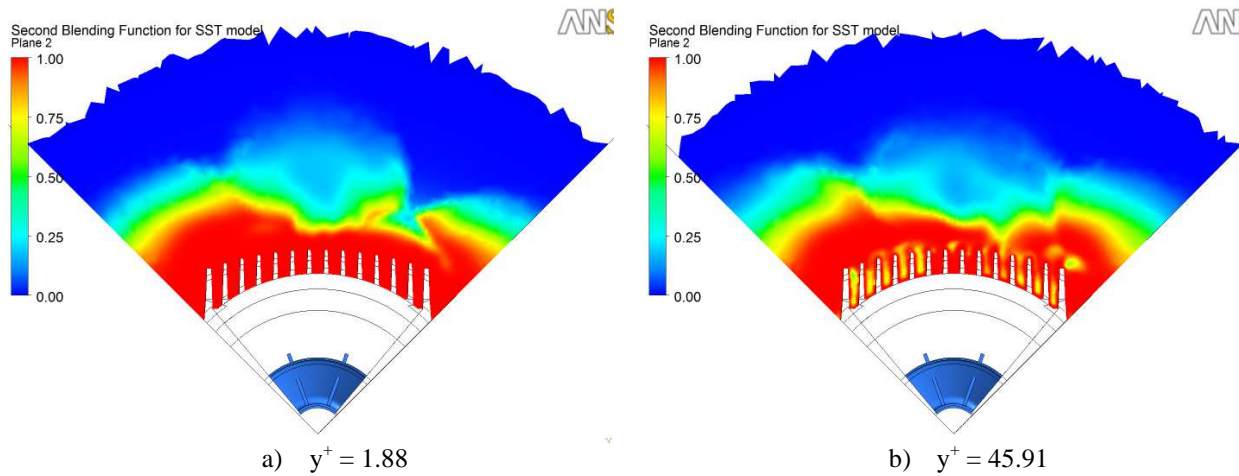


Figure 14: distribution of $k-\omega$ and $k-\epsilon$ turbulence models in a plane

CONCLUSIONS

These conclusions are valid for this problem and respective boundaries conditions.

The proposed methodology allowed addressing the efforts to the aspects associated with the numerical problem, eliminating doubts related to the geometric aspects. As a result, the parameters that are essential for the study of the airflow on the external surface of electric motors were obtained.

Considering average air velocity per plane, this evaluation showed similar results for k- ϵ and SST, however results obtained with k- ϵ are in most cases over predicted, fact that may become a big problem in industrial applications.

During the preliminary simulations, the SST turbulence model presented a much superior robustness than the k- ϵ model, since some simulations with k- ϵ resulted in the crashing of the software.

The small differences verified with different configurations of layers prisms are attributed to Automatic Wall Treatment and SST, but the ideal y^+ value should be respected ($y^+ \leq 2$);

ACKNOWLEDGMENT

The authors want to thank WEG, for the support and testing facilities and ESSS (Engineering Simulation and Scientific Software), for the support to ANSYS-CFX.

BIBLIOGRAPHY

- [1] C. A. Cezario, Análise do Escoamento do Ar em Motores de Indução Totalmente Fechados, UFSC, **2007**.
- [2] F. R. Menter – Zonal Two Equation k- ϵ Turbulence Models for Aerodynamic Flows, AIAA Paper 93-2906, **1993**.
- [3] W. Vieser, T. Esch, F. Menter, Heat Transfer Predictions using Advanced Two-Equation Turbulence Models. CFX Validation Report: CFX-VAL10/0602, CFX, **2002**.
- [4] ANSYS CFX, ANSYS CFX, Release 13.0 – Help Guides. ANSYS Europe Ltd. **2011**.
- [5] CFX-TASCflow, Theory Documentation, version 2.12, AEA Technology Engineering Software Ltd, Canada, **2002**.
- [6] Cl. R. Maliska, Transferência de Calor e Mecânica dos Fluidos Computacional, LTC, Rio de Janeiro, **2004**.